Proceedings of the 17th World Congress
The International Federation of Automatic Control
Seoul, Korea, July 6-11, 2008

BACKSTEPPING BASED APPROACH FOR CONTROLLING SPACECRAFT MICRO PUMP FOR PROPULSION SYSTEM

C. S. Teodorescu*, H. Siguerdidjane*, A. Arzandé*, P. Gebbers*, J-C. Vannier*, F. Roux**

**SUPELEC, 3 Rue Joliot-Curie, 91192 Gif-sur-Yvette, France*
*** CSTM, 31320 Castanet- Tolosan, France*

Abstract: The purpose of this paper is to design a robust controller for the new design of hydrazine micro pumps, by studying the real prototype using a high-performance oscilloscope attached to the real pump system. In other words we have designed a relatively accurate mathematical model of the micro pump by using the data extracted with the oscilloscope and then we have calculated and tested a robust controller using backstepping technique. Simulation results are satisfactory regarding the desired criteria. The micro pump consists of an electromagnetic actuator which moves a piston forward and backward (stroke 0 to a few mm). The main advantage in using these new devices consists on increase the capacity maneuverability of the satellite with the same tank volume gain with respect to the existing satellites systems allowing the overall system to operate even if the gas reservoir pressure level is low, thus bringing great advantages (reduced costs, better maneuverability).

Keywords: Nonlinear control systems, modeling, propulsion system, satellite.

1. INTRODUCTION

Research in the satellites technology has been increasing in the last years as more exploration space vehicles have been sent out and the planned space missions have increased, emphasizing the interest in this field in the near future, throughout the world. Thus scientists are continuously working on developing new design models, with reduced size and weight, having enhanced capabilities and better overall performance. Using the acquired experience throughout the last years, the new criteria in terms of performance, robustness and long lifetime can be achieved by intensifying the practical and theoretical investigations related to space vehicles, including planetary Landers together with their newly developed specific propulsion systems. Details on different propulsion systems may be seen, for example in (Griffin and French, 1991, Hill and Peterson, 1965).

In this paper, we emphasize our research connected to small satellites technologies. The starting point in our research concerns the gas tank which cannot be totally emptied, resulting a considerable amount of used gas, because the currently designed system does not have the physical capability to operate for low pressure values inside the reservoir, that is, below a given value it is not possible to apply any impulse control even though the gas tank has fuel in it and that is the end of the satellite usual lifetime. In order to improve the lifetime of the propulsion system, a new concept consists of using a micro pump with hydrazine gas for which a prototype has been conceived and realized.

Therefore, the goal of this paper is to design a robust controller for this new design of hydrazine micro pumps, by means of mathematical modeling, control and simulation results, in order to test the proposed solution with respect to a number of physical constraints.

The concept of the micro pump is based on an electromagnetic actuator by which it is possible to move the piston forward and backward (due to the

fluid pressure) and thus transferring fuel with a desired frequency from accumulator to tank. The position of the running piston in normal functioning mode should be in the range of 0 to a few mm. In some previous work (Vannier *et al*., 2003), one may find the details of the technology involving the actuator, in addition to some heuristic but operating controllers. Some stabilization problems arise related to these controllers in some frequencies range that are difficult to handle, but the fact that no analytic analysis is yet available needs to be taken into account. Previous studies stress upon the undesirable vibrations that appear when using open loop controller. This is a reason for choosing to elaborate a more accurate mathematical model of the micro pump system. Using this model we have been able to design a robust, but complex controller. Depending on the constraints regarding the complexity of the real controller, it might be possible to simplify the mathematical form of one that we propose, nevertheless affecting the overall robustness.

In order to improve the operating required range of frequencies, the modeling of the micro pump has been revisited and unlike the one described in (Vannier *et al.,* 2005), in the newly model we take into account the changes of pressure in the tankers. The mathematical modeling phase is a very difficult task because, for the physical experimentations, we obviously could not use the hydrazine, so we have used water or Nitrogen gas instead.

We have then applied the backstepping based approach in order to make the system robust with regards to some vibrations that might occur in the real system. For more than a decade, this approach has become very popular with respect to nonlinear systems in the "strict feedback form". We have been able to successfully apply it on the calculated system of equations regarding the model of the micro pump and afterwards we have performed the numerical simulations which showed that the overall micro pump system met the desired criteria (operating frequency, oscillating amplitude) throughout both transient and steady state regime. Early studies stress on the problems that arise with classical controller designs in the transient regime (Vannier *et al*., 2003).

The paper is organized as follows. Section 2 describes the basic principal of the system under consideration. Section 3 is dedicated to the proposed revisited nonlinear modeling. The controller design is derived in Section 4. In Section 5, we have attached the simulation results. A short conclusion ends the paper.

2. MICRO PUMP BASIC PRINCIPLE

The described micro pump operates with an assumed linear reluctance motor as actuator. It has a cylinder-shaped stator that accommodates the translator and exhibits rotational symmetry (Arzandé, *et al.*, 2002). The translator consists of a shaft whose movement is confined on both sides: on one side, a circular disk with the same diameter as the stator acts as a magnetic conductor and on the other side, there is a smaller disk with a rubber damper. The translator enters a pressure chamber that is equipped with two valves so that the linear movement of the translator is transformed into pumping action. This part might be referred to as the moving circular diaphragm, namely a disk of thickness *a* with a hole in its centre where the pump axis is rigidly fixed.

The stator of the actuator accommodates the coil of *n* turns, placed perpendicular to the magnetic field that is wound around the axe of the translator. When a current flows through the coil, a magnetic field is built up that flows through the stator and the translator. The advantage of using an electromagnet over a normal one consists on the ability to vary the magnetic field.

The system acts to minimize its magnetic energy. Since most of the energy is stored in the gap between the big stopper disc and the stator, it results a force that strives to close the gap. The force can be described as:

$$F_{magn} = \frac{dE}{dx} \tag{1}$$

with E as the magnetic energy and x as the position of the translator. The magnetic energy of the system is given by:

$$E = L(x)\frac{I^2}{2} \tag{2}$$

which renders the magnetic force:

$$F_{magn} = \frac{dL(x)}{dx}\frac{I^2}{2} \tag{3}$$

The actuator structure exhibits a rotational symmetry. The axis of symmetry is displayed in dashed line as illustrated in figure 1. I denotes the electrical current which flows in the coil. h is the height of the slot. e is the air gap thickness, r_1 and r_4 are the actuator interior and exterior radius respectively while r_2, r_3 are the interior and exterior slot radius respectively.

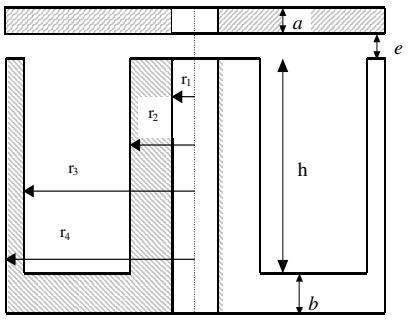

Fig.1. Actuator scheme of CSTM

The material of the actuator's magnetic core has been chosen so that the magnetic flux passing trough the coil would meet a sufficiently high frequency for the pump flow and a relative good amplitude level of the magnetic field, providing the force capable to drive forward and backward the translator. Previous studies concerning the materials used, the calculation of the different forces involved in this system together with the physical constraints, the induced voltages and current levels have been carried out and described in (Dugué *et al.*, 2000, 2001). The prototype of the micro pump is shown in figure 2.

Fig.2. Pump prototype (Copyright CNES 2000)

3. MODELING

Consider the scheme below:

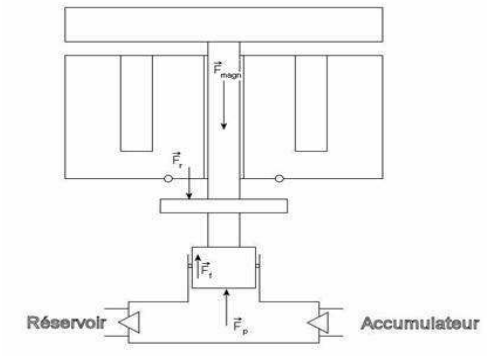

Fig.3. Pump scheme

Roughly speaking, during pumping action, two main forces are involved: the magnetic force, and the force from the pressurized system. Whenever the magnetic force is low, the translator is pushed away from the pressure chamber by the pressure of the liquid, the valve of the liquid reservoir opens and the chamber gets filled. The contrary movement happens when the current in the coil rises and the magnetic force gets stronger: the stator moves towards the chamber, the second valve opens whereas the first one closes, and the liquid is pressed into the accumulator. This leads to an increase of the pressure in the accumulator. The pressure force F_{pres} was modeled assuming ideal valves, with instantaneous pressure changes:

$$F_{pres} = \begin{cases} F_{res} & (\text{if } \dot{x}_1 < 0) \\ F_{acc} & (\text{if } \dot{x}_1 > 0) \end{cases} \tag{4}$$

where

$$F_{res} = \frac{1 - sign(x_2)}{2} P_{res} A$$

and

$$F_{acc} = \frac{1 + sign(x_2)}{2} P_{acc} A$$

In the formulas above we have considered the Ox axis as given in figure 3, x_1 being the position and x_2 being the speed of the piston.

Other forces that appear in the model are as follows: the translator's movement in the stator is subject to friction that is modeled according to Coulomb friction:

$$F_f = x_2 f \tag{5}$$

When the gap closes all the way we have a physical metal-to-metal contact, namely the *metal-bumper force* F_{mb}, modeled as a linear spring with very high coefficient a_b:

$$F_{mb} = a_b x_1 \sigma_1 \tag{6}$$

where

$$\sigma_1 = \begin{cases} 1, & if\ x_1 < 0 \\ 0, & if\ x_1 \geq 0 \end{cases}$$

This limiting force should take high values for x_1 decreasing in the vicinity of zero. The metallic bumper should not be touched by the piston in order to avoid undesired vibrations and the damage of the pump's subparts.

The pump has a second elasto-plastic bumper on the other extremity. For determining a simple model of this bumper, the static force-to-strain curve has been experimentally measured and approximated by a 3rd order polynomial. The *elasto-plastic bumper force* is thus modeled as a nonlinear spring:

$$F_{pb} = \left(a_{h0} x_1^3 + a_{h1} x_1^2 + a_{h2} x_1 + a_{h3}\right) \sigma_2 \tag{7}$$

where

$$\sigma_2 = \begin{cases} 1, & if\ x_1 > x_{1h} \\ 0, & if\ x_1 \leq x_{1h} \end{cases}$$

x_{1h} being the upper limit of the free piston movement, where the rubber bumper has been placed (figure 4, with normalized scales).

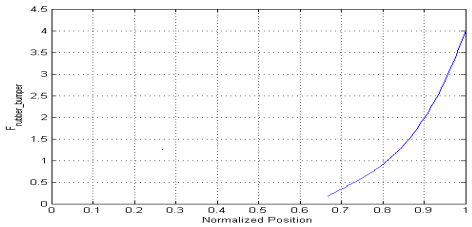

Fig.4. Nonlinear spring model of F_{pb}

To calculate the inductance, the system has been modeled using *Force Electromotive* modeling. The inductance has been approximated by the function:

$$L(x) = L_0 + \frac{L_1}{x_1^2} \tag{8}$$

making the magnetic force:

$$F_{magn} = -\frac{L_1 I^2}{x_1^3} \tag{9}$$

The piston micro pump weight is neglected, so when applying Newton's second law we have:

$$m\ddot{x}_1 = F_{acc} + F_{res} + F_{magn} - F_f + F_{mb} - F_{pb} \tag{10}$$

The resulting system in state space representation is:

$$\begin{cases} \dot{x}_1 = x_2 \\ \dot{x}_2 = \dfrac{1}{m}\begin{pmatrix} \dfrac{1+sign(x_2)}{2}P_{acc}A + \dfrac{1-sign(x_2)}{2}P_{res}A \\ -\dfrac{L_1 I^2}{x_1^3} - x_2 f + a_b x_1 \sigma_1 \\ -\left(a_{h0}x_1^3 + a_{h1}x_1^2 + a_{h2}x_1 + a_{h3}\right)\sigma_2 \end{pmatrix} \\ \dfrac{dI}{dt} = \dfrac{1}{L(x_1)}\left(U + 2\dfrac{L_1}{x_1^3}x_2 I - RI\right) \end{cases} \tag{11}$$

The coil is supplied using the variable voltage U. By applying the Faraday's law (differential) and the Kirchoff loop rule and taking into account the loss resistance R in series to the coil, we get

$$U = \frac{d\left(L(x_1(t))\cdot I(t)\right)}{dt} + RI \tag{12}$$

By extracting the derivative of the current, we get the third equation of the overall system.

A simplified scheme of the power converter which has been used is given in figure 5. It consists of two MOS Transistors T_1 and T_2, plus two diodes D_1 and D_2. V represents its input voltage source.

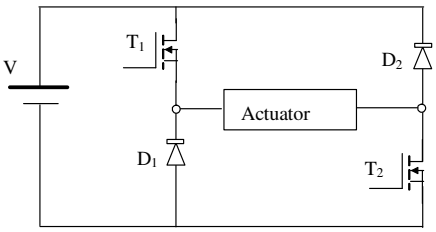

Fig.5. Input power converter

Simulating the free evolution of the newly designed micro pump model, we get the following graphic:

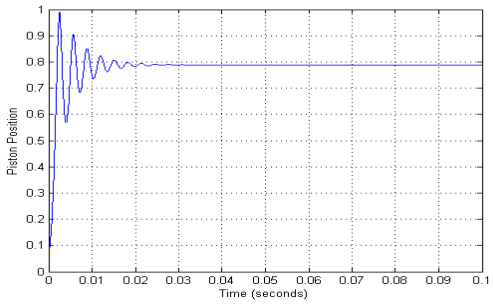

Fig.6. Normalized free evolution of the piston position

4. CONTROLLER DESIGN

Consider the first two equations of the system, with x_1 and x_2 as the state variables and $C = I^2$ the command. Because this subsystem is in the "strict feedback form", we can apply backstepping technique in order to calculate the desired current value I. Using this information and the 3rd equation of the system, one may be able to extract the desired values of the voltage U. Finally we have the mathematical form of U that we need in order to control the micro pump's piston. The normalized constraint $U \in [-1, 1]$ has been taken into account.

4.1 Position reference trajectory

Consider $\phi_0(t)$ as being the desired trajectory function for x_1 in the following form:

$$\phi_0(t) = A_1 \sin(2\pi\nu t + \psi) + \frac{x_{1\max} - x_{1\min}}{2} \tag{13}$$

where A_1 is the amplitude of the reference signal, ν is the frequency, $x_{1\max}$ and $x_{1\min}$ are the upper and lower maximum physical limits reachable by the piston and $\psi = \psi(x_{1\,ini})$ is chosen so that $\phi_0(t_0) = x_{1\,ini}$, with t_0 the initial time. Should the initial position of the piston $x_{1\,ini}$ exceed the range of $\phi_0(t)$, we may apply an initial voltage impulse on the pump in order to have $x_{1\,ini}$ within the reach of

$\phi_0(t)$. Note that ϕ_0 is centered in the middle of the admissible range of x_1.

4.2 Trajectory tracking using backstepping based approach

Using the first equation, ϕ_0 as reference trajectory for the first state variable x_1, and the Lyapunov function:

$$V_1(\varepsilon_1) = \frac{1}{2}\varepsilon_1^2 > 0,\ \varepsilon_1 = x_1 - \phi_0 \qquad (14)$$

we have been able to calculate the virtual command for the second state variable x_2 by imposing the negative-definite condition on V_1, resulting:

$$\phi_{x2}(x_1) = \dot{\phi}_0 - k_1(x_1 - \phi_0),\ k_1 > 0 \qquad (15)$$

For the second step of backstepping, we have used the second equation of the model, ϕ_{x2} as reference for x_2 and the Lyapunov function:

$$V_2(\varepsilon_1, \varepsilon_2) = V_1(\varepsilon_1) + \frac{1}{2}\varepsilon_2^2 > 0, \qquad (16)$$

with $\varepsilon_2 = x_2 - \phi_{x2}$

Finally we got the final formula for the command by imposing the negative-definite condition on V_2, resulting: $\phi_c \leftarrow C = I^2$

$$\varphi_C = \frac{m(x_1)^3}{L_1}\begin{pmatrix} \frac{\beta}{m} - \ddot{\varphi}_0 + (k_1 + k_2)(x_2 - \dot{\varphi}_0) \\ +(1 + k_1 k_2)(x_1 - \varphi_0) \end{pmatrix} \qquad (17)$$

with $\beta = \begin{pmatrix} \sigma_3 - x_2 f + a_b x_1 \sigma_1 \\ -\left(a_{h0}x_1^3 + a_{h1}x_1^2 + a_{h2}x_1 + a_{h3}\right)\sigma_2 \end{pmatrix}$

$k_1 > 0$ and $k_2 > 0$ are parameters used, according to the Lyapunov function, to control the sensibility and the time response of the overall system.

4.3 Command U

Using the third equation of (11), we get

$$U = \left(L_0 + \frac{L_1}{x_1^2}\right)\frac{dI}{dt} - 2\frac{L_1}{x_1^3}x_2 I + RI \qquad (18)$$

5. SIMULATION RESULTS

5.1 Simulation results without perturbation

A set of numerical simulations has been performed and the values of the parameters used have been normalized in the figures hereafter.

The position and the current signals are given in figures 7 and 8 respectively. One may observe that the system perfectly tracks the reference trajectory. The position doesn't reach the upper constraint and the current intensity remains within the required physical bound. The voltage across the windings is shown in figure 8. One may also notice that it is within the normalized interval $U \in [-1, 1]$. The frequency of the reference signal is $\nu = 140Hz$.

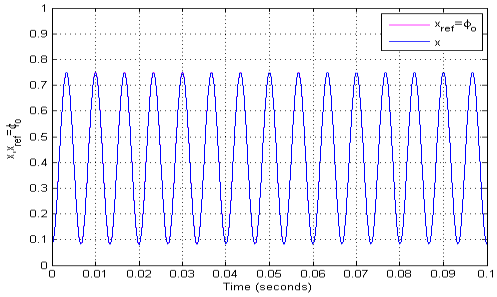

Fig.7. Piston normalized position and reference trajectory

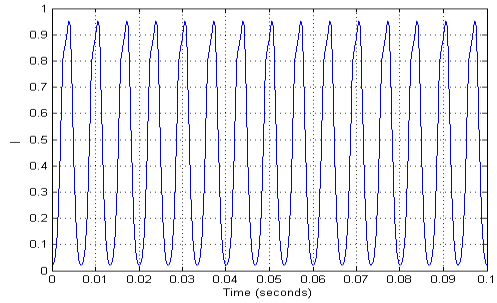

Fig.8. Normalized current intensity

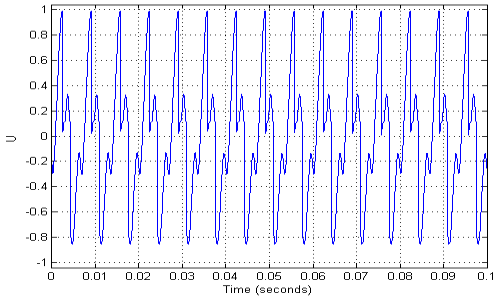

Fig.9. Normalized voltage across the windings

5.2 Simulation results with unstructured uncertainties

Consider an external unknown perturbation force acting on the piston and having the physical meaning of spontaneous external vibration acting on the micro pump itself and thus on the piston. If the induced force may be assumed as $W = m\delta_x$, δ_x might be considered as the acceleration of the perturbation force acting on the piston. We have used the range $\delta_x \in [-7, 7]$ and the Uniform Random block of

Simulink. The perturbation lasts for 0.1 seconds starting from $t_0 = 0.1$ seconds (figure 10).

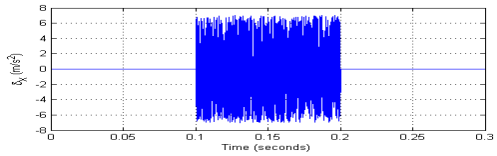

Fig.10. Sample δ_x

Figures 11-13 show the position, the current and the voltage signals respectively. Similarly, one may also observe that the system perfectly tracks the reference trajectory in spite of the applied uncertainties. The tracking error is given in figure 14 in the presence of the perturbation for finite time-interval [0.1 0.2] seconds.

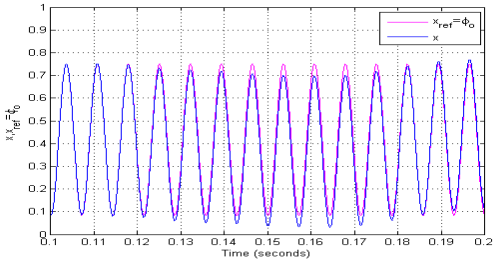

Fig.11. Piston normalized position and reference trajectory

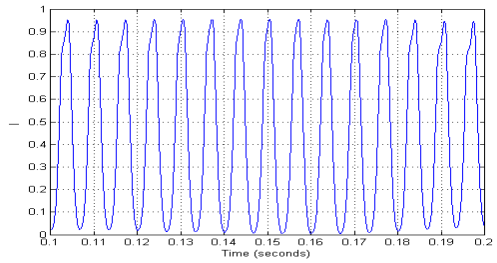

Fig.12. Normalized current intensity

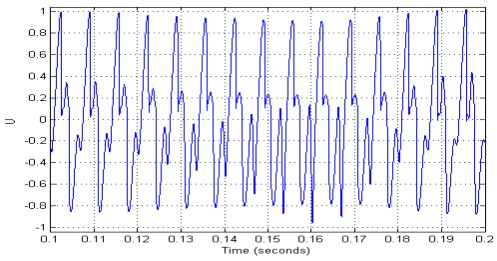

Fig.13. Normalized voltage across the windings

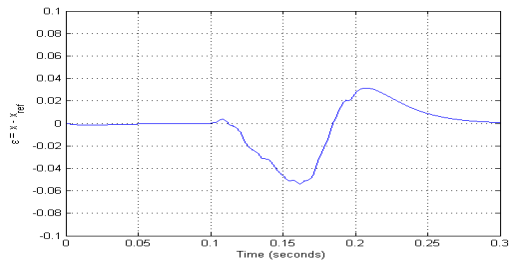

Fig.14. Normalized tracking error- with perturbation

6. CONCLUSION

This paper presents a revised modeling of a new design hydrazine micro pump for small satellites propulsion systems, taking into account the pressure changes for increased validity of the model. A set of numerical simulations have been performed and have proved that the proposed controller, based on backstepping approach, leads to satisfactory results even in the case of high frequency range for the reference signal. Also, we have achieved good performance in terms of robustness with regards to unstructured uncertainties.

REFERENCES

Griffin M. D., French J. R. (1991). Space Vehicle Design, *AIAA Education Series*.

Hill P.G., Peterson C. R. (1965), *Mechanics and Thermodynamics of propulsion.* Addison-Wesley, Reading, MA.

Vannier J-C, P. Vidal, P. Dessante and F. Dugué (2003). Optimisation d'un ensemble convertisseur, actionneur électrique et pompe pour un système d'alimentation en carburant. *Electrotechnique du Futur*, Gif-sur-Yvette, pp. 110.

Arzandé A., F. Dugué, J-C Vannier and P. Vidal (2002). Actionneur électrique rapide de pompe à carburant: modélisation, simulation dynamique et système de commande. *Aerospace Energy Equipment Conference*, Avignon.

Dugué F., Roux F., Bonafos B., Billard J-Y., Fruman D.H., Gibek I (2000). Hydrazine Propulsion Systems with a Micro pump Spacecraft Propulsion. *International Conference* N°**3**, Cannes, France.

Dugué F., B. Bonafos, J-C. Vannier and P. Vidal (2001). Actionneur linéaire rapide, conception, simulation et essais, *Electrotechnique du Futur*, Nancy, pp. 42-48.

Vannier J-C, A. Arzandé, H. Siguerdidjane, P. Vidal and F. Dugué (2005). Control of a new hydrazine pump generation in propulsion system. *16th IFAC World Congress*, Prague.

AKNOWLEGMENTS

This study has been carried out within a research work related to CNES interests, through the company CSTM.